THE EFFECT OF REINFORCEMENT DETAILING IN RC WALLS ON THE BEHAVIOUR OF DCM BUILDINGS WITH WALL STRUCTURAL SYSTEM

UTICAJ METODE ARMIRANJA AB ZIDOVA NA PONAŠANJE ZGRADA SREDNJE DUKTILNOSTI SA ZIDNIM KONSTRUKTIVNIM SISTEMOM

UDC:
Original Scientific Paper

Radomir FOLIĆ, (corresponding author)[1]
Zoran BRUJIĆ [2]
Boris FOLIĆ[3]
Miloš ČOKIĆ [4]

ABSTRACT

In this paper, a wall structural system building (acc. to EC8), with reinforced concrete (RC) walls is analysed. The focus is on analysing the system post-elastic behaviour, using the nonlinear static and dynamic analysis methods. Three models (each with different RC wall reinforcement detailing) are used for the comparative analysis of the building behaviour. The results of this analysis are used to compare the response of buildings with the walls designed according to EC8 (with boundary elements) and buildings with uniformly distributed rebar in the RC wall cross-section. Walls are modelled as column-rigid beam elements with fiber nonlinear hinges, but with different distribution and quantities of the reinforcing steel in each model. The model with RC walls that have "boundary" elements modelled as a part of the wall is chosen as a referent model for comparative analysis with the other two models. Based on the results of nonlinear analysis methods some conclusions and recommendations are given.

***Key words**: Building structures, RC walls, nonlinear seismic analysis, boundary elements, stirrups, rebar detailing methods*

REZIME

U ovom radu, analizirani su konstruktivni sistemi zgrada sa armirano-betonskim (AB) zidovima sa fokusom na njihovo post-elastično ponašanje, primenom metoda nelinearne statičke i dinamičke analize. Tri modela zgrada sa različitim detaljima armiranja AB zidova su analizirana i upotrebljena za uporednu analiza seizmičkog odgovora zgrade. Rezultati analize su iskorišćeni za upoređenje odgovora zgrada, na seizmička dejstva, sa zidovima projektovanim prema EC8 (koji sadrže ivične elemente) i zgrada sa ravnomerno raspoređenom armaturom u poprečnom preseku AB zidova. Zidovi su modelirani kao sistemi stubova i krutih greda sa vlaknastim modelima plastičnih zglobova, ali sa različitim rasporedom i količinama armature u sva tri modela. Kao referentni model za komparativnu analizu, odabran je model sa AB zidovima koji imaju ivične elemente. Na osnovu rezultata dobijenih primenom metoda nelinearne analize, date su odgovarajuće preporuke.

***Ključne reči**: Konstrukcije zgrada, AB zidovi, seizmička nelinearna analiza, ivični elementi, uzengije, metode armiranja*

Adresa autora: 1 Dr. Ing. Professor Emeritus, University of Novi Sad, Faculty of Technical Sciences, Department of Civil Engineering, Trg Dositeja Obradovića 6, Novi Sad, Serbia
E-mail: folic@uns.ac.rs
2 Dr. Ing. Assoc. Professor, University of Novi Sad, Faculty of Technical Sciences, Department of Civil Engineering, Trg Dositeja Obradovića 6, Novi Sad, Serbia
E-mail:zbrujic@uns.ac.rs
3 Dr. Ing. University of Belgrade, Innovation Centre, Faculty of Mechanical Engineering, Kraljice Marije 16, Belgrade, Serbia
E-mail:boris.folic@gmail.com
4 PhD student, University of Novi Sad, Faculty of Technical Sciences, Department of Civil Engineering, Trg Dositeja Obradovića 6, Novi Sad, Serbia
E-mail: cokicmilos@gmail.com

1. INTRODUCTION

Modelling of a structural system can be a very complex process, depending on the complexity of the system and the software package that is used. The accuracy of the analysis depends on adopted theoretical assumptions, input parameters and their reliability. The calculation consumption time is correlated with the analysis methods applied and the complexity of the structural model. Within a structural system of the building, RC walls are generally modelled in the following two ways (Figure 1):

– System of two frame elements – A column with geometric characteristics of the wall; a beam or link ele-

ment with very high stiffness properties (Figure 1a). In this approach, the modelling process of nonlinear hinges is very complex. The accuracy of the results and calculation time are dependant to a certain extent on the modelling accuracy of nonlinear hinges.

– Shell elements – The modelling process is simpler. Walls are modelled as multi-layered shell elements (Figures 1b and 2). The accuracy of the results and calculation time are dependant to a certain extent on the density properties of 2D finite elements grid.

In both cases, rigid beams (Figure 1b) have 100 times higher flexural stiffness (*EI/L*) and 100 times lower axial stiffness (*EA*) than the "regular" beams connected to the wall. Imbedded beams do not have nonlinear hinges.

The modelling of walls as a multi-layered shell element or frame element system, was analysed by Kubin

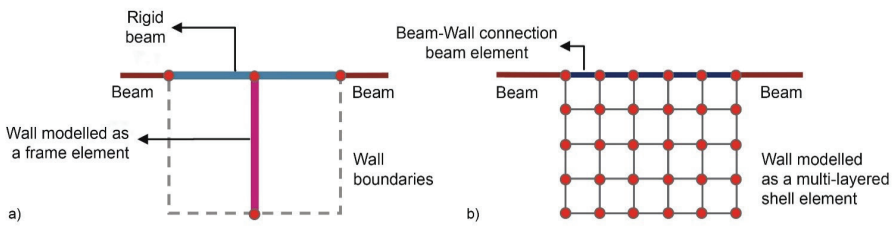

Figure 1. Wall models: a) frame elements system; b) shell element (acc. to Fahjan Y. M. et al. 2010)

J. et al (2008), Fahjan Y. M. et al. (2010), Ajmal M. et al. (2015), Sukumar B. et al. (2016) on the 3D (spatial) model of the structure. Ajmal M. et al. (2012), Fahjan Y.

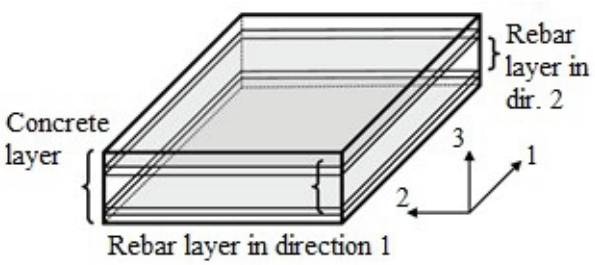

Figure 2. Multi-layered shell element (acc. to Fahjan Y. M. et al. 2010)

M. et al. (2012) did a comparative analysis on 2D (plane) model of a building frame. Based on the results of their research, it can be concluded that modelling of walls with frame elements will give similar results compared to structures with shell wall-element models, but with more or less accuracy, depending on the analysed structure.

Oh Y.-H. et al. (2002) studied the effect of boundary element details of structural walls on their deformation capacities. Structural walls considered in their study had different sectional shapes of boundary element details, with barbell-shaped RC wall as well. In this study, only rectangular RC walls were considered. As expected, wall specimen without boundary elements has shown the lowest performance parameters, compared to other specimens.

In their research, Darani F.M. and Moghadam A.S. (2012) investigated the effect of wall aspect ratio, axial force, and boundary element characteristics on the behaviour of low-rise shear walls. Response parameters included maximum lateral strength, lateral displacement at maximum strength and failure mode of walls.

In his research, Hoult R.D. (2017) investigated, at that moment, current and proposed longitudinal reinforcement requirements of the Concrete Structures code in Australia (AS 3600). He analysed RC wall using FEM software for a range of different longitudinal reinforcement configurations. The research showed better performance of RC walls with boundary elements, compared to the walls with evenly distributed reinforcement and also, a better performance of the walls with the larger quantity of evenly distributed reinforcement compared to lightly reinforced walls with evenly distributed reinforcement.

Lu Y. and Henry R.S. (2015) tested six walls to investigate the seismic behaviour of RC walls with distributed minimum vertical reinforcement in accordance with provisions in NZS 3101:2006. They developed detailed numerical models of lightly RC walls to understand the behaviour of the test walls, and to investigate the performance of walls with minimum vertical reinforcement. Results from these analyses showed that wall size, reinforcement type and concrete strength had a significant effect on the cracking behaviour and lateral drift capacity of RC walls.

In their paper, Berely A. et al. (2018) were focused on the development of the tools that would enable obtaining of the performance states (PBEE) of load-bearing walls. The in-plane behaviour of the slender RC walls

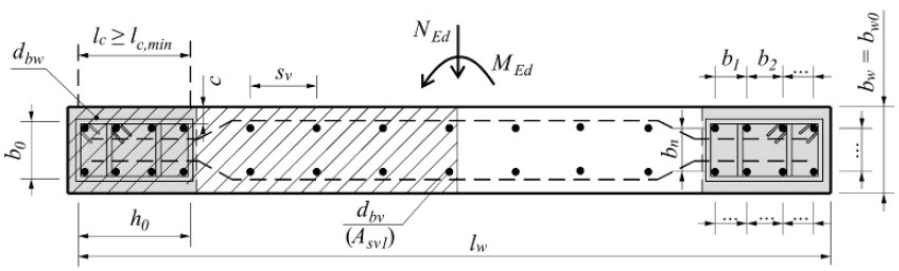

Figure 3. Rectangular cross-section RC wall with boundary elements (M1), (acc. to Milev J., 2016)

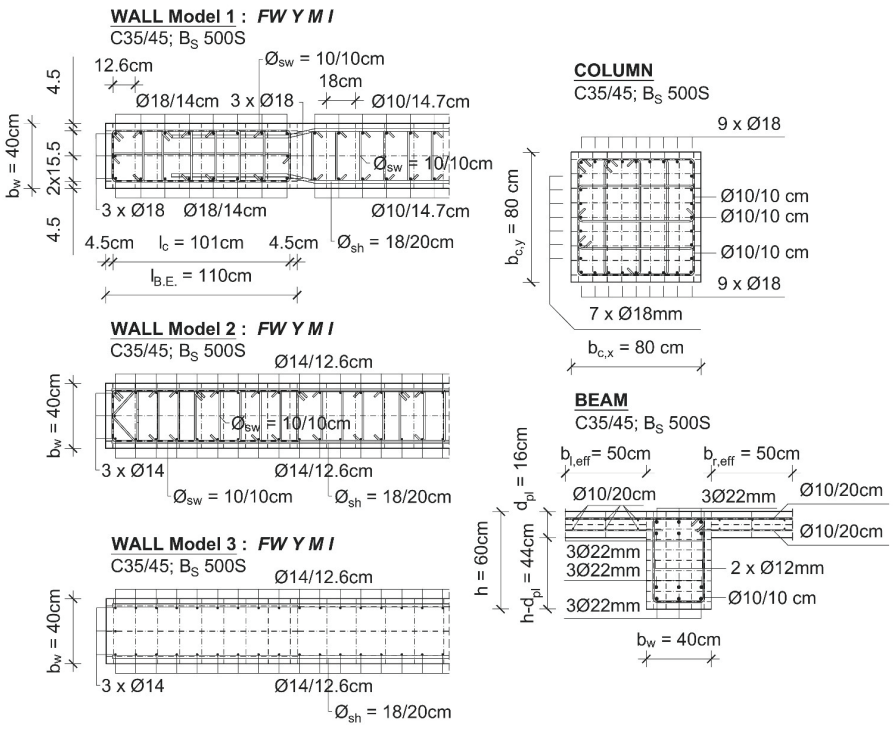

Figure 4. Reinforcement detailing in RC walls, columns and beams

was analyzed. Necessary preparations for the experimental research, its realization and the role in design of tall buildings are presented in the paper. This provides a basis for the adequate simulations and designed RC walls with the different configurations.

In the paper by Menegon S. J. et al. (2018), the aspect of the introduction of the ductility factor for RC walls, related to the practical detailing approach, is widely discussed. The comparison with the assumed values in the performance analysis according to AS 1170.4 is given as well.

In the research by Gallardo J. A. et al. (2018), the initial point is the fact that the buildings with load-bearing walls behaved favourably in the recent earthquakes, including Chile, in 2010, and the damages were mainly concentrated on the ground floor. Several computational models have been developed to analyze the fracture mechanisms and behaviour of the RC walls. It is noted that the micro-models were simulating the distribution of the stress and strain really well. A case study of an 18-storey building that was seriously damaged in the 2010 Chile earthquake is presented in detail and a nonlinear time history analysis was applied. The proposed model for the prediction of the structural behavioural has shown satisfactory accuracy. The case study allows the assessment of the damping effects in non-ductile structures and it indicates the importance of the stiffness of RC plates on the structural response to vertical ground excitation.

In his paper, Milev J. (2016) discussed the problems and solutions in the design of RC wall structures, and among them, the local ductility requirements and checks after (EN1998-1). "*Local ductility of ductile walls can be ensured by providing the confined boundary elements in the critical zone of the wall. However the procedure for calculation of the length of confined boundary elements is complicated and is partly clear in Eurocode 8 even for the case of walls with rectangular cross section. In author's opinion the procedure is iterative even for the simple cases.*" (Figure 3)

In this paper, three mathematical models (M1, M2, M3) were used, in order to analyse and compare the behaviour of DCM wall structural system (EN1998-1) that contain RC walls with and without boundary elements (Figure 4). Cross sections of RC wall (*FW Y M I*), columns and beam (*B Y3*) and division grid of fibers are shown in Figure 4.

The main difference between the wall M1 and walls M2 and M3 is the different position and quantity of the rebar in wall-elements. RC walls in M1 are designed according to (EN1998-1), (EN1992-1) as the walls with boundary elements (Figure 4). M2 and M3 have RC walls without boundary elements (Figure 4) and they are compared to the referent model M1. RC walls in M2 are designed as fully confined RC walls and RC walls in M3 are designed as fully unconfined RC walls, but with the same amount of vertical reinforcement as in M2. With the exclusion of boundary elements, all other propositions given in (EN1998-1), (EN1992-1) were adopted in their design. Geometrical characteristics (length, width, height) of the walls are the same in all three models.

The results of this analysis are used to compare the behaviour of a wall structural building system with – and without boundary elements in RC walls and the effect of equal reinforcement distribution in RC walls without boundary elements on the post-elastic behaviour of the structure. Nonlinear static analysis (NSA) and nonlinear dynamic analysis (NDA) methods were used in the analysis of the structural system behaviour. NSA method was used to perform pushover analysis. Seven different accelerograms obtained from (Ambraseys N., 2002), (ORFEUS) and cyclic load testing pattern for shear resistance of vertical elements for buildings (ASTM E2126) were used while performing NDA. To fully observe the behaviour of the structures in post-elastic zone, global displacements, inter-story drifts (IDR) and cyclic testing values were used for the comparative analysis.

2. MATERIALS AND METHODS

2.1. Geometric and material properties of the structure

The subject of the analysis is an office-residential building with 11 levels (basement, ground floor + 9 stories). The structural system of the building is a wall system (EN1998-1). The main structural elements of the analysed structure are RC slabs, walls, beams and columns. The raster of the structure is shown in Figures 5 and 6. The length of one span in the longitudinal (X) direction is 4.8 m (8x4.8 m total), and in the transverse direction (Y) 5.4 m (5x5.4 m total).

The height of basement and the ground floor is 3.6 m, while the height of the other 9 stories is 3.2 m, so the total height of the building is 36.0 m. In order to simplify the modelling and calculation process, all vertical elements are fixed at the bottom level of the structure, i.e. soil-structure interaction is not included in the calculation and design.

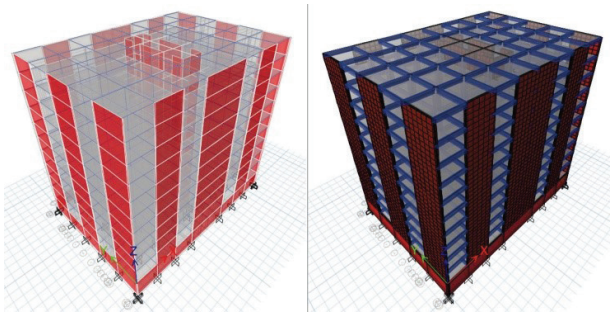

Figure 5. Linear analysis model

Material properties of concrete C35/45 (EN1992-1) and reinforcing steel class C (f_{yk} = 500 MPa, k = 1.15) (EN1992-1) have been adopted for model analysis. The structure is designed for the medium ductility class (DCM) behaviour (EN1998-1).

The structural design is done according to the European building design standards (EN1998-1), (EN1992-1), (EN1990) and (EN1991), and the calculations are performed using (ETABS). The structural behaviour is analysed by performing NSA and NDA methods. The N2 method (EN1998-1) is used for the calculation of target displacement values.

The position of the walls in the structural system is shown in Figure 6. Geometric characteristics of the cross-section properties of the walls are shown in Table 1.

Table 1. Geometric characteristics of structural elements

Level	Basement – 10th story	Wall length on all floors	L_W (full/B.E/I.E) [m]
Plate: d_{pl} [cm]	16	FW X L	10.0 / 1.8 / 6.4
Beams: b_w/h [cm]	40/60	FW X S	5.2 / 1.0 / 3.2
Columns: d_x/d_y [cm]	80/80	FW Y E, FW Y M, CW Y	5.8 / 1.1 / 3.6
Walls: b_w [cm]	40	CW X UE	4.4 / 0.9 / 2.6
		CW Y UE	2.2 / 0.7 / 0.8

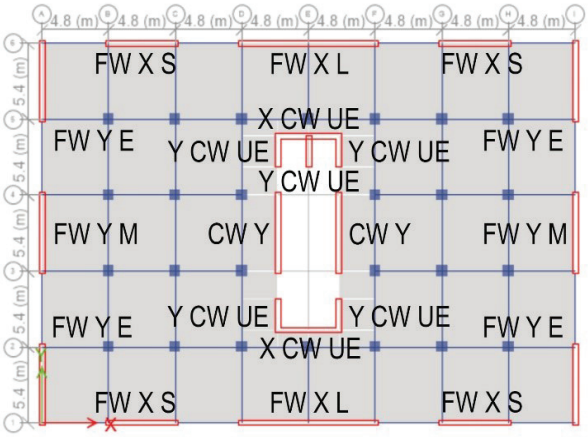

Figure 6. Walls position – plan view

The calculations of the structure are done according to the methodology and recommendations given in (EN1998-1), (EN1992-1), (EN1990) and (EN1991). There are two phases of modelling and calculation process for the building structure analysis. The first phase includes the creation and analysis of the model M0 that is used for linear-elastic analysis of the structure and design of elements. The second phase includes the creation of three building models (M1, M2 and M3) with different RC wall elements. M1-M3 was used for the analysis of post-elastic behaviour of the structure and comparative analysis of the results.

The first structural model M1 is the referent model, where RC walls are modelled with boundary elements (Figures 3 and 4). The remaining two models are used for a comparative analysis with M1. In M2 and M3, the same required quantity of rebar is evenly distributed in each wall (Figure 4), but the main difference between the models is that walls in M2 are fully confined while M3 walls are fully unconfined RC elements.

2.2. Loads and actions

The applied loads are as follows: permanent loads (G_i) – self-weight of structural elements and an additional permanent load; live load (Q_i) and seismic load (S_i). Load combinations and design values of actions for calculations are used according to (EN1992-1).

2.2.1. Vertical load

There are two different types of vertical loads on the construction: the weight of the structural elements and the additional permanent load (G_i) and the variable-live load (Q_i). The adopted value of the permanent constant load is g_{pl} = 3.0 kN/m^2 on all floors. The load intensity of the variable-live load amounts to q = 3.0 kN kN/m^2 (EN1991) on all floors, except on the roof slab at which the load intensity is equal to q_r = 1.0 kN/m^2 (EN1991). The

self-weight load of façade elements, which is imposed on all façade beams except the roof façade beams is equal to g_f = 10.0 kN/m on beams and 3.0 kN/m on RC walls. The value of the reduction factor of the live loads is $\psi_{2,i}$ = 0.3 (EN1992-1).

2.2.2. Horizontal (seismic) action

To calculate the peak ground acceleration (*PGA*) action on the structure, an elastic response spectrum (RS), type 1 (EN1998-1) is used, for ground type C (EN1998-1). The reference *PGA* for reference return period of the reference seismic action for the no-collapse requirement T_R = 475 years, with reference probability of exceedance of P_R = 10 % in 50 years, which amounts $a_{gR} = 0.2 \cdot g$ was chosen. Since the building has an office-residential function, it corresponds to the class of importance II, for which the value of the importance factor is γ_I = 1.0 (EN1998-1), so calculated value of the *PGA* is equal to $a_g = 0.2 \cdot g$ (EN1998-1). The adopted damping value is 5%, after (EN1998-1). For more about damping please see (Ćosić M. et al., 2017). Eccentricity ratios of 5% for both directions are included. The maximum and the adopted value of the behaviour factor is q = 3.0 (EN1998-1).

Seismic base shear force for each horizontal direction is calculated with the correction factor value λ = 0.85 (EN1998-1). Elastic and design response spectrums are shown in Figure 7.

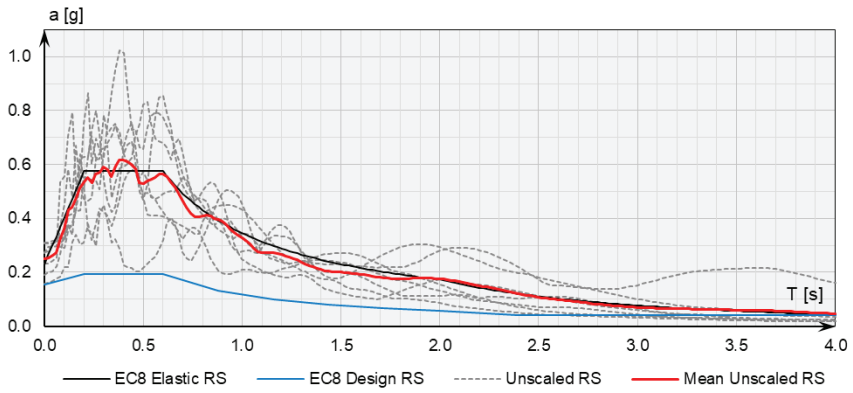

Figure 7. Elastic and design RS and unscaled TH data

Table 2. Main properties of the earthquakes that were used in NDA

Name	Earthquake	Station ID/Code	Date/Time	M_W	Original PHA [cm/s^2]
EQ01	Alkion, Greece	121	24.02.1981/20:53:39	6.6	303.630
EQ02	Umbria, Italy	221	26.09.1997/09:40:30	6.0	195.100
EQ03	Izmit, Turkey	472	17.08.1999/00:01:40	6.6	303.770
EQ04	Central Italy	CNE	30.10.2016/06:40:18	6.6	288.280
EQ05	Modena, Italy	MOG0	29.05.2012/07:00:02	5.9	167.075
EQ06	Adana, Turkey	0105	27.06.1998/13:55:53	6.2	271.955
EQ07	Modena, Italy	MIR08	29.05.2012/07:00:02	5.9	242.970

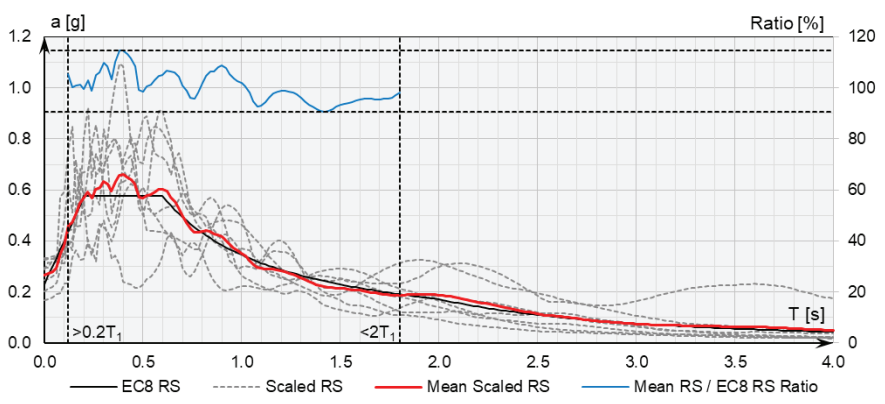

Figure 8. Elastic RS, scaled TH data, mean scaled RS and their differences

In order to perform NDA, 7 different accelerograms were selected (Figure 7). The criteria for time-history data selection was that magnitude M>5.5Ms (Type 1 RS (EN1998-1)), the records correspond to soil Type C and $v_{s,30}$ = 180 – 360 m/s (Ambraseys N., 2002), (ORFEUS). In addition, records from (ORFEUS) are obtained using *REXELite* tool that allows searching for a suite of waveforms compatible with a target spectrum, generated according to (EN1998-1). Selected earthquake data is shown in Table 2.

Two different methods were applied to analyse the nonlinear behaviour of the system through NDA. In the first case, time-history data was scaled (Figure 8) with the common scale factor F_S = 1.07, which was obtained using the least square method (LSM). In the second case, accelerograms were matched using (Figure 9) (SeismoMatch, 2018). Both methods are described in detail in (Ćosić M. and Brčić S., 2012), (NIST GCR 11-917-15). In the first case, when scaled time-history (TH) data is used, dispersion of the results should give the higher range of obtained values, while in the second case, when matched time-history data is used, the results values should be closer to the mean value. Both mean RS (scaled and matched) satisfy the (EN1998-1) provisions,

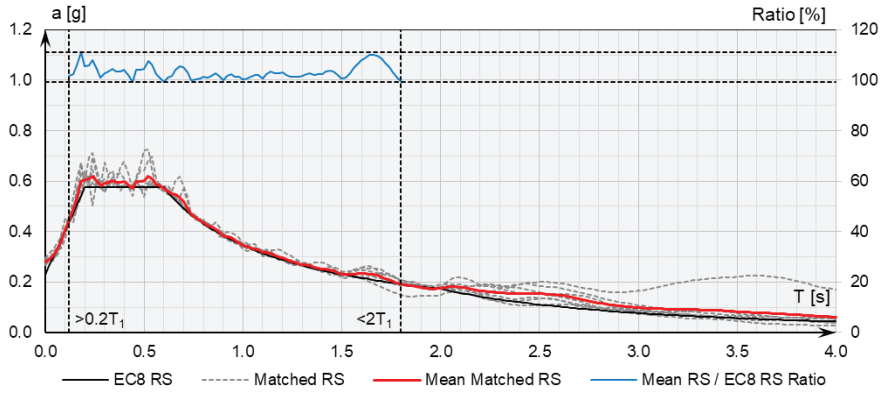

Figure 9. Elastic RS, matched TH data, mean matched RS and their differences

where mean RS should not be below 90% value of the elastic (EN1998-1) RS at any point in range of $0.2 \cdot T_1$ – $2 \cdot T_1$, and $a_g(T_0) \cdot S$ of (EN1998-1) RS should be lower than $a_g(T_0)$ of mean RS.

2.3. Adopted properties and simplifications of structural modelsd

A spatial (3D) model is used for the structure's analysis, which is conducted in (ETABS). The following parameters, assumptions and simplifications are adopted:

– RC plates are horizontally rigid diaphragms

– Second-order (P-Δ) effects are included in the calculation

– Cracked structural elements properties are included in the calculation

– Elastic flexural and shear stiffness properties of all RC elements (walls, columns, beams and plates) are reduced to 50% for element design. (EN1998-1)

– Torsional stiffness is calculated as 10% of elastic torsion for element design. (EN1998-1)

– Wall finite-element (FE) mesh is rectangular, with the maximum distance of 1 m between the FE nodes.

– In all RC walls, flexural stiffness, induced by the shear horizontal in-plane force, is reduced to 50% of its elastic stiffness (EN1998-1), (Bisch P., 2011)

– In all RC walls, bending stiffness in out-of-plane direction is reduced to 10% of its elastic stiffness (EN1998-1), (Bisch P., 2011)

– The shear stiffness of all RC walls with cracked properties is reduced to 50% of its elastic stiffness (EN1998-1), (Milev J. and Kardziev V., 2012)

– All perimeter basement walls have full linear-elastic behaviour (Rana R. et al. 2004)

– Inner basement walls have the same properties as their corresponding ground floor walls, except perimeter basement walls, which are designed as linear-elastic elements.

2.4. Linear-elastic analysis model

Linear-elastic structural model M0 was used for the design of structural elements. All RC walls are designed according to (EN1998-1), (EN1992-1). That process is described in (Milev J. and Kardziev V., 2012) for the building that had DCM behaviour. Fardis et al. (Fardis M. N. and Tsionis G., 2011) is also used in the walls design process.

2.5. Nonlinear analysis model

In addition to parameters, assumptions and simplifications that are used for all models, for the post-elastic analysis models, the following are used as well:

– structural elements are modelled with material properties for nonlinear behaviour of concrete (EN1992-1), (Mander J. et al., 1988) and reinforcing steel (EN1992-1) (Figure 10)

– The behaviour of RC is described by a Takeda hysteretic model and the Kinematic model of hysteresis was used for the reinforcement. Both models are an integral part of the software package (ETABS).

– elastic flexural stiffness properties reduction for the walls, beams and columns from linear-elastic model are excluded from the calculation, because their behaviour will be determined by P-M-M hinges and constitutive relationships shown in Figure 10,

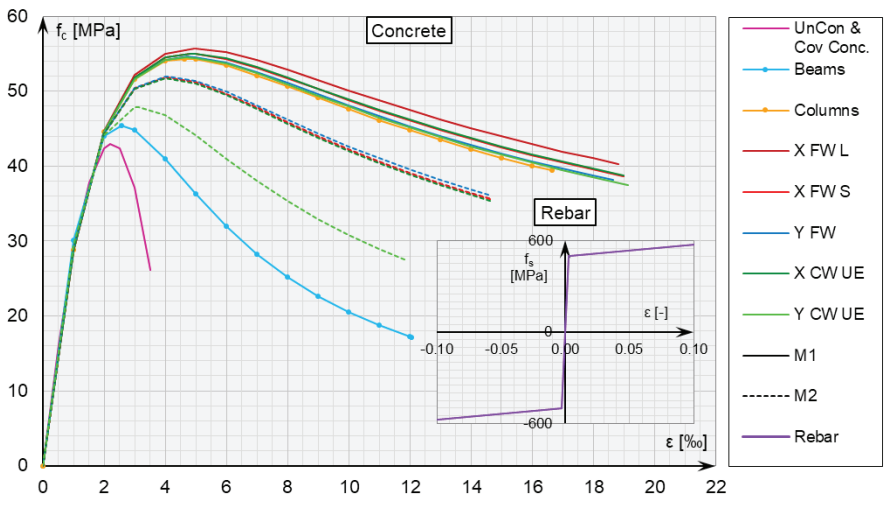

Figure 10. Materials stress-strain relationship

– elastic shear stiffness properties reduction for the walls (for in-plane actions) from linear-elastic model is excluded from the calculation, because its behaviour will be determined by shear hinges and constitutive relationships shown in Figure 12,

– effective flange widths are considered in nonlinear analysis and were calculated according to (EN1998-1). The width of the effective beam flange is equal to 50 cm on the side of the beam.

2.6. Nonlinear hinge properties

The properties of confined concrete in structural elements are calculated according to (Mander J. et al., 1988). The stress in concrete is described by the equation:

$$f_c = \frac{f_{cm,c} \cdot x \cdot r}{r - 1 + x} \tag{1}$$

where

$$x = \frac{\varepsilon_c}{\varepsilon_{cm,c}} \tag{2}$$

ε_c is compression concrete strain. $f_{cm,c}$ is maximum compressive strength value of confined concrete and $\varepsilon_{cm,c}$ is corresponding compression concrete strain. ε_{cm} is equal to:

$$\varepsilon_{cm} = \varepsilon_{c2} \cdot \left[1 + 5 \cdot \left(\frac{f_{cm,c}}{f_{cm}} - 1 \right) \right] \tag{3}$$

where f_{cm} = 43 MPa (C35/45) is unconfined concrete maximum compressive strength and ε_{c2} = 2‰ (EN1992-1) is its corresponding strain value. E_c (EN1992-1) and E_{sec} are tangent and secant concrete elasticity modules in the equation:

$$r = \frac{E_c}{E_c - E_{sec}} \tag{4}$$

and

$$E_{sec} = \frac{f_{cm,c}}{\varepsilon_{cm,c}} \tag{5}$$

Ultimate strain value in confined concrete core $\varepsilon_{cu,c}$ is calculated according to expression given in (Paulay T. / Priestley M.J.N., 1992):

$$\varepsilon_{cu,c} = 0.004 + 1.4 \cdot \frac{\rho_{yh} \cdot f_{yh} \cdot \varepsilon_{su}}{f_{cm,c}} \tag{6}$$

where volumetric ratio of confining reinforcement ρ_{yh} is calculated according to simpler and safe-sided equation which considers that essentially the minimum of the two transverse reinforcement ratios (ρ_{wx}, ρ_{wy}) controls confinement (Fardis M. N., 2009):

$$\rho_{yh} = 2 \cdot \min(\rho_{wx}, \rho_{wy}) \tag{7}$$

f_{yh} is the yield stress of confining reinforcement and ε_{su} is the ultimate strain of confining reinforcement.

Plastic hinges are modelled as fiber cross sections. Nonlinear behaviour of structural elements (walls, columns and beams) is modelled with nonlinear plastic hinges. P-M-M nonlinear fiber hinge models are used to analyse the effects of axial forces and bi-directional moments on nonlinear behaviour of the system.

In many investigations, the influence of the lateral load on the RC walls nonlinear shear behaviour is neglected or included through the reduced elastic shear stiffness of those elements. In (EN1998-1), both bending moments and shear forces are not computed directly from the seismic actions obtained in the analysis, but from the capacity design approach. This approach is used to ensure that the beginning of formation of flexural nonlinear hinges will be in the lower part of RC walls and that shear strength of RC walls exceeds the value needed to develop the wall's flexural strength (Booth E., 2014).

This is achieved by using the tension shift which is the vertical, parallel upper shift increasement of the design moments that have been already increased by the formation of linear design-moment function from ground floor to the roof. In addition, shear magnification factor of ε = 1.5 is used for the multiplication of design shear force envelopes in DCM systems. For DCH systems, this procedure is more complex (Fardis M. N., 2009), (Booth E., 2014), (Avramidis I., 2016). As a result of this procedure, it is necessary to reinforce the walls in upper floors with more flexural and shear rebar than it would be required if the effects were processed directly from the seismic actions.

In this design approach, it is only allowed to develop a single plastic hinge at the base and the walls must act as vertical cantilevers. By preventing the formation of plastic hinges in the wall at the upper stories, the elastic part of the wall tends to behave almost as a rigid body above the flexible zone of the hinge at the base, maintaining relatively uniform inter-storey drifts throughout the height of the building (Eurocode Standards).

This procedure leads to flexure over strengthened RC walls (Figure 11) which can affect the property of the structure to have a stiff response at the design PGA and also to reach its full ductile potential at the higher PGA intensities than for the value of the design PGA.

Eurocode 8 has special design provisions for systems consisting of several large but lightly reinforced RC walls, sustaining seismic demands not by dissipating seismic energy through hysteresis in plastic hinges, but by converting part of it into potential energy of the masses due to upward displacements and returning another part to the ground by radiation from their foundation (Fardis M. N., 2009).

However, the building in M1, M2 and M3 do not qualify as a "system of large lightly reinforced walls" by failing to meet one of the conditions, in which the fundamental period in each horizontal direction cannot be higher than 0.5 s and all its primary walls should be designed as DCM walls (Fardis M. N., 2009).

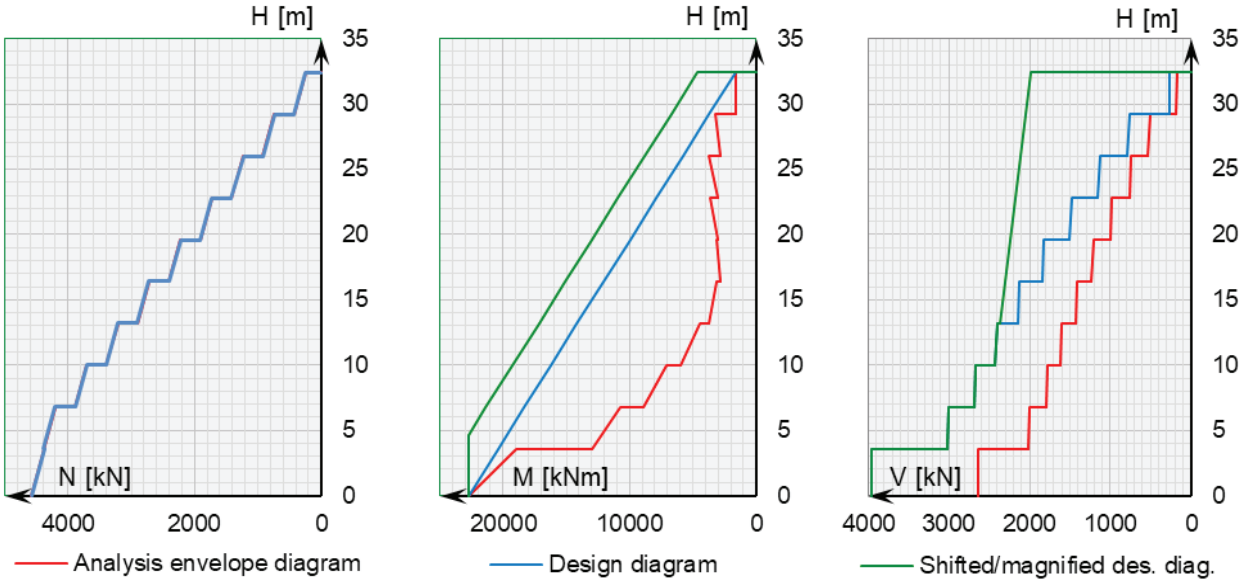

Figure 11. RC wall (FW Y M I) analysis and design diagrams

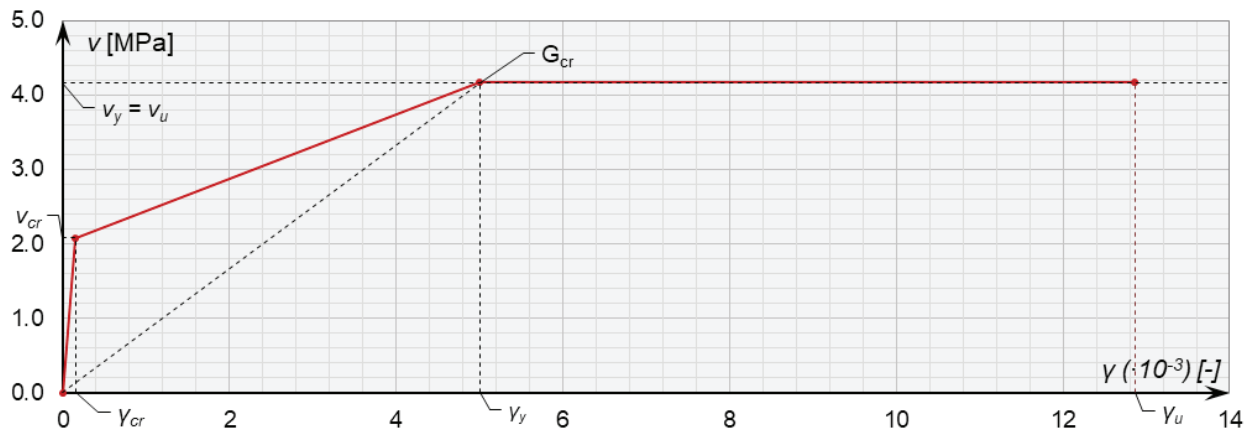

Figure 12. Shear hinges stress-strain relationship in wall FW Y M I

Contrary to the approach where only P-M-M hinges were included to model the nonlinear behaviour of ductile RC walls, shear hinges were also included to model RC walls behaviour. The method that was applied is described in (Gerin M. & Adebar P., 2004), (Hagen G. R., 2012). Shear hinge model stress – strain relationship in wall *FW Y M I* is shown in Figure 12. The same methodology was applied for other RC walls.

To obtain shear hinge model, it is necessary to calculate the values shown in Figure 12. Cracking shear stress v_{cr} is equal to the lesser value of (Gerin M. & Adebar P., 2004), (ACI 318-11):

$$v_{cr} = \begin{cases} N \geq 0; \min\left(f_{cr} \cdot \sqrt{1 + \frac{n}{f_{cr}}}, 0.27 \cdot \sqrt{f_c'} + 0.25 \cdot \frac{N}{A_c} \right) \\ N < 0; \min\left(f_{cr} \cdot \sqrt{1 + \frac{n}{f_{cr}}}, 0.17 \cdot \sqrt{f_c'} + 0.29 \cdot \frac{N}{A_c} \right) \end{cases} \quad (8)$$

where f_{cr} represents the principal tensile stress at cracking, which can be estimated as (Gerin M. & Adebar P., 2004):

$$f_{cr} = 0.33 \cdot \sqrt{f_c'} \quad (9)$$

where f'_c is represents the compressive strength of concrete. The shear strain at the start of the formation of the cracking γ_{cr} in the wall is calculated by the expression:

$$\gamma_{cr} = \frac{v_{cr}}{G} \quad (10)$$

and the value of elastic shear modulus is calculated according to (ACI 318-11):

$$G = 0.4 \cdot E_c \quad (11)$$

where E_c is concrete elastic modulus. According to (Gerin M. & Adebar P., 2004), (ACI 318-11), (Zhao X, 2011)

the value of cracked section shear stiffness G_{cr} is defined as the secant stiffness to the yield point:

$$G_{cr} = \frac{\nu_y}{\gamma_y} \tag{12}$$

The shear stress at yield ν_y and the ultimate shear stress ν_u are assumed to be equal to the shear strength obtained using (ACI 318-11) expressed as a shear stress (Figure 12):

$$\nu_y = \nu_u = min\left(\alpha_c \cdot \sqrt{f_c'} + \rho_h \cdot f_y \le 0.25 \cdot f_c', 0.83 \cdot \sqrt{f_c'}\right) \tag{13}$$

where coefficient α_c is equal to:

$$\alpha_c = \begin{cases} 0.17; h_w/l_w \ge 2.0 \\ lin.int.[0.17, 025]; 1.5 \ge h_w/l_w \ge 2.0 \\ 0.25; h_w/l_w \ge 1,5 \end{cases} \tag{14}$$

The shear strain of reinforced concrete at the yield point γ_y can be determined from the following simple strain transformation:

$$\gamma_y = \varepsilon_h + \varepsilon_v - 2 \cdot \varepsilon_{45} = \frac{f_{ys}}{E_s} + \frac{\nu_y - n}{E_s \cdot \rho_v} + \frac{4 \cdot \nu_y}{E_c};$$

$$0 \le \frac{\nu_y - n}{E_s \cdot \rho_v} \le \frac{f_{ys}}{E_s} \tag{15}$$

where ε_h and ε_v represent the normal strains in the horizontal and vertical reinforcement directions and ε_{45} is the strain at 45° to the reinforcement and in the direction closest to the principal compression strain direction. f_{ys} is the reinforcement yield stress and E_s is the reinforcement modulus of elasticity. n represents the vertical axial compression and ρ_v is the vertical reinforcement ratio. Conservative limit on the shear strain ductility μ_y proposed in (Gerin M. & Adebar P., 2004) is calculated using the equation:

$$\mu_y = \frac{\gamma_u}{\gamma_y} = 4 - 12 \cdot \frac{\nu_y}{f_c'} \tag{16}$$

and the value of the ultimate shear strain γ_u can be obtained using the following expression:

$$\gamma_u = \mu_\gamma \cdot \gamma_y \tag{17}$$

Column and beam P-M-M plastic hinges are located at the 15% and 85% of the element clear span, with the plastic hinges length of 0.3L, where L is a clear length of the element. RC walls have P-M-M plastic hinges, which are located at the 15% of and 85% element total height, on all floors except the basement, ground and 1st floor, with the plastic hinges length of 0.3L, where L is a clear length of the element. Dominant nonlinear behaviour of RC walls is usually expected in the first two floors (ground and 1st floor) (Milev J. and Kardziev V., 2012). For that reason, on these stories, the distributed plasticity approach was used, which means that each wall on the basement, ground and 1st floor have 5 P-M-M hinges that are distributed along their full length. These hinges have the same length of 0.2L, but they are located at the 0.1L; 0.3L; 0.5L; 0.7L and 0.9L of the element total height. Shear hinges are modelled as a shear stress and strain function ($\nu - \gamma$). They are located on 0.5L on each wall on which P-M-M plastic hinges are modelled and they integrate the entire section across its height in the calculation.

Among several expressions (Zhao X. et al., 2011), the commonly used equation given by (Paulay T. & Priestley M.J.N., 1992) was used for the calculation of the plastic hinge length, because of its application simplicity:

$$L_{pl} = 0.08 \cdot L + 0.022 \cdot f_y \cdot d_{bL} \ge 0.44 \cdot f_y \cdot d_{bL} \tag{18}$$

where L_{pl} is a plastic hinge length, $L = M/V$ is a shear span, f_y is longitudinal rebar yield stress and d_{bL} is a mean value of longitudinal rebar diameter.

2.7. Modelling of the structural elements

RC walls, columns and beams have nonlinear properties. The walls are modelled as nonlinear column – rigid beam elements (Figure 1). Each wall section is defined with many fiber sections (Figure 4), whose behaviour is described using constitutive stress – strain relationship functions (Figures 10 and 12).

Rebar quantities in walls, columns and beams, used in analysed models are presented in Tables 3 and 4. Rebar quantity is calculated based on the wall model design:

– M1 – design with confined boundary elements (Figure 4). Wall models in M1 are designed according to (EN1998-1), (EN1992-1), (Milev J. & Kardziev V., 2012) from the results obtained in M0, for a DCM structural behaviour (EN1998-1). Wall models include confined boundary elements at the ends (Figure 4) and unconfined element between them (Figure 4). This model is used as a referent (comparison) model.

– M2 – model with reinforcement quantity calculated (with ETABS) according to (EN1998-1), (EN1992-1), for evenly distributed bars (Figure 4). This model is fully confined along its length.

– M3 – model with the same rebar quantity as in M2, but this model is fully unconfined along its length.

Indexes *I*, *II* and *III* in Table 3 represent the story position of RC walls. Index *I* refers to basement, 1st floor and 2nd floor. Index II refers to RC walls placed in 3rd, 4th and 5th floor. Index II refers to RC walls positioned from 6th to 10th floor.

The modelling of core walls is done by designing the each wall segment of the core according to design actions in nonlinear analysis. They are modelled as a group of multiple column-rigid beam elements.

The reinforcement in columns and beams is the same in M1, M2 and M3. The focus of the paper is to analyse the effect of walls reinforcement detailing on behaviour of RC building. In this way, the reinforcement in beams and columns did not affect the differences in structural system's behaviour between the models and has no direct impact on difference of the results in the compara-

Table 3. Reinforcement quantity in RC walls

Wall	Vertical reinforcement		Confinement		Shear reinforcement
Model	**M1 (B.E. / I.E.)**	**M2, M3**	**M1**	**M2**	**M1, M2, M3**
Properties	**(n_{bL}) d_{bL} / s_{bL}** [mm/cm]	**Whole RC wall** [mm/cm]	**($n_{sw,d}$ / $n_{sw,b}$) d_{sw} / s_{sw}** [mm/cm]		**d_{sw} / s_{sw}** [mm/cm]
FW X L I	(32)Ø20/12.00 / (84)Ø10/15.10	(138)Ø16/14.75	(3 / 15) Ø10/10	(2 / 68) Ø10/10	Ø20/20
FW X L II	(32)Ø18/12.01 / (84)Ø10/15.10				Ø18/20
FW X L III	(32)Ø16/12.03 / (84)Ø10/15.10	(138)Ø14/14.76			Ø16/20
FW X S I	(18)Ø16/12.63 / (40)Ø10/13.00	(74)Ø14/14.53	(3 / 8) Ø10/10	(3 / 36) Ø10/10	Ø16/20
FW X S II	(18)Ø12/12.69 / (40)Ø10/13.00				Ø14/20
FW X S III					Ø12/20
FW Y E I	(18)Ø22/13.97 / (48)Ø10/14.74	(94)Ø16/12.63	(3 / 8) Ø10/10	(3 / 46) Ø10/10	Ø18/20
FW Y E II	(18)Ø18/14.03 / (48)Ø10/14.74	(94)Ø14/12.64			Ø14/20
FW Y E III	(18)Ø14/14.09 / (48)Ø10/14.74				
FW Y M I	(18)Ø18/14.03 / (48)Ø10/14.74	(94)Ø14/12.64	(3 / 8) Ø10/10	(3 / 46) Ø10/10	Ø18/20
FW Y M II					Ø14/20
FW Y M III	(18)Ø14/14.09 / (48)Ø10/14.74				
CW Y I	(18)Ø14/14.09 / (48)Ø10/14.74	(94)Ø14/12.64	(3 / 8) Ø10/10	(3 / 46) Ø10/10	Ø14/20
CW Y II					
CW Y III					Ø12/20
CW X UE I	(18)Ø12/11.26 / (36)Ø10/14.06	(62)Ø14/14.78	(3 / 8) Ø10/10	(3 / 30) Ø10/10	Ø16/20
CW X UE II					
CW X UE III					Ø14/20
CW Y UE I	(14)Ø12/11.76 / (12)Ø10/13.40	(32)Ø14/14.90	(3 / 6) Ø10/10	(3 / 15) Ø10/10	Ø12/20
CW Y UE II					
CW Y UE III					Ø10/20

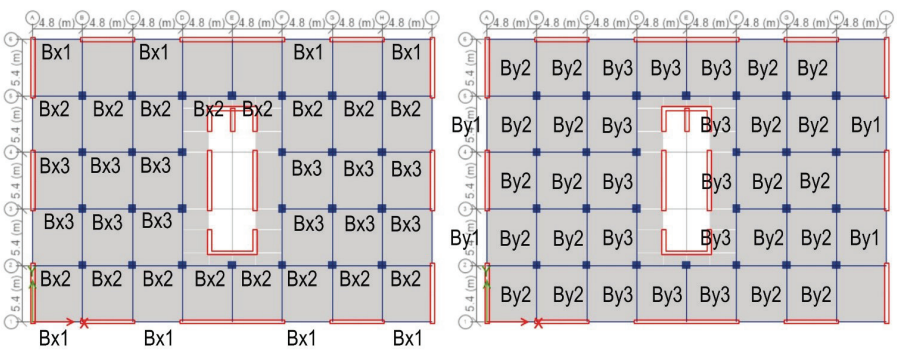

Figure 13. Beam positions – plan view

Table 4. Reinforcement quantity in columns and beams

Level		**Basement – 10th story**				
Reinforcement		**Flexural**				**Confinement/Shear**
Columns:		32 – Ø18				Ø10/10
Beams:		**Flexural**				**Confinement/Shear**
B_{X1}	*top*	6 – Ø25	**B_{Y1}**	*top*	6 – Ø25	Ø10/10
	bottom	6 – Ø25		*bottom*	5 – Ø25	
B_{X2}	*top*	5 – Ø22	**B_{Y2}**	*top*	3 – Ø25	Ø10/10
	bottom	5 – Ø22		*bottom*	3 – Ø25	
B_{X3}	*top*	3 – Ø25	**B_{Y3}**	*top*	6 – Ø22	Ø10/10
	bottom	3 – Ø25		*bottom*	6 – Ø22	

tive analysis. The reinforcement amount in columns and beams by their position (Figure 13) are shown in Table 4. All columns have the same amount of reinforcement. Representation of the reinforcement detailing in RC walls, columns and beams is shown in Figure 4. Fibers division that was used for plastic hinges modelling is as well shown in the structural cross-sections in the Figure 4.

3. RESULTS AND DISCUSSION

3.1. Modal analysis

The load dependant Ritz (LDR) vector is used for the modal analysis in the linear-elastic design and NSA models. It converges faster and more uniformly than Eigen vectors (ETABS).

Rayleigh mass (M) – tangential stiffness (K_T), viscous damping was applied in the NDA. The damping matrix of the system is a combination of mass and stiffness matrices and it is shown by the following equation:

$$[C] = \alpha_M \cdot [M] + \alpha_K \cdot [K_T] \tag{19}$$

where $[C]$, $[M]$ and $[K_T]$ are damping, mass and tangential stiffness matrices, respectively. Parameters α_M and α_K represent the proportional coefficients of damping of mass and stiffness.

The value of T_1 corresponds to the first translational periods in the X or Y direction or the first rotational period R. The value of T_2 corresponds to the translational periods in the X or Y direction or the rotational period R, which refers to the period value in which the structural system reaches at least 90% of the sum of effective modal masses in one of the 2 translational directions or one rotational direction. The structure is torsionally stiff. Values of the periods used are shown in Table 5.

Table 5. Periods of vibration of the structure

MODEL	T_{M1} [s]	m_{M1} [%]	T_{M2} [s]	m_{M2} [%]	T_{M3} [s]	m_{M3} [%]
Y_1	0.868	66.64	0.871	66.64	0.860	66.64
Y_2	0.079	91.12	0.079	91.10	0.078	91.19
X_1	0.674	67.26	0.678	67.24	0.666	67.38
X_2	0.069	91.11	0.069	91.09	0.068	91.17
R_1	0.583	65.53	0.586	65.52	0.577	65.64
R_2	0.053	90.38	0.053	90.36	0.052	90.46

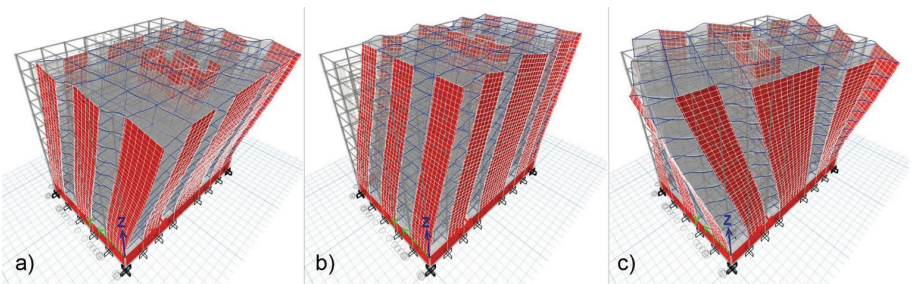

Figure 14. First three fundamental periods of vibration of the structure: a) T_1 – translation (Y dir.); b) T_2 – translation (X dir.); c) T_3 – rotational PROMENI

3.2. Nonlinear static pushover analysis

3.2.1. Pushover curves

A NSA is performed for both main (X and Y) directions. Two different load distribution patterns are used for the analysis: mass proportional (PROP) and modal (MOD). PROP load distribution is the mass-proportional load distribution and modal (MOD) represents the 1st mode load distribution for appropriate direction. The results of NSA for both directions are shown in Figure 15.

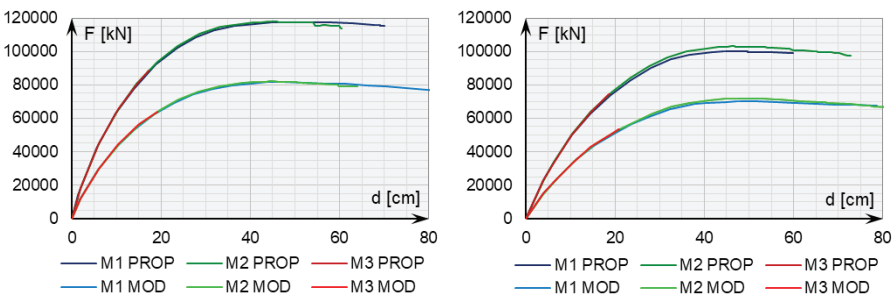

Figure 15. Pushover curves in X (left) and Y direction (right)

Based on NSA results (Figure 15), it is evident that there is a negligible difference in the behaviour of three building models until a certain point. The main difference M1, M2 and M3 can be spotted "deep" in the non-linear zone. While M1 pushover curve has a "smooth" shape until the last calculated value, a small stiffness drop is noticeable in M2 in the last calculated points, before the calculation is ended by the non-convergence of the solution. However, M3 reaches its ultimate capacity point much earlier, compared to the first two models, which is expected, because there is no confinement in the RC walls. That leads to overall, lower ductility of the walls and the structure and inability of the walls to receive the stresses which may be absorbed by the confined RC walls in M1 and M2. The full discussion of the results of the analysis from the aspect of displacements, global and inter-story-drifts is given in the paper by Čokić et al. (2021).

3.3.2. Global drifts, inter-story drifts and damage limitations

Values of global drifts (GDR) and inter-story drifts (IDR) obtained in NDA for PGA of 0.2*g* are shown in Figures 16-19. Minimum, mean and maximum global GDR values and percentage differences of their highest values in M2 and M3, compared to M1 are shown in Tables 6-9. The range in differences is bigger in the case when scaled TH data was used in the analysis, which was expected, based on the wider PGA range in scaled than in matched TH data.

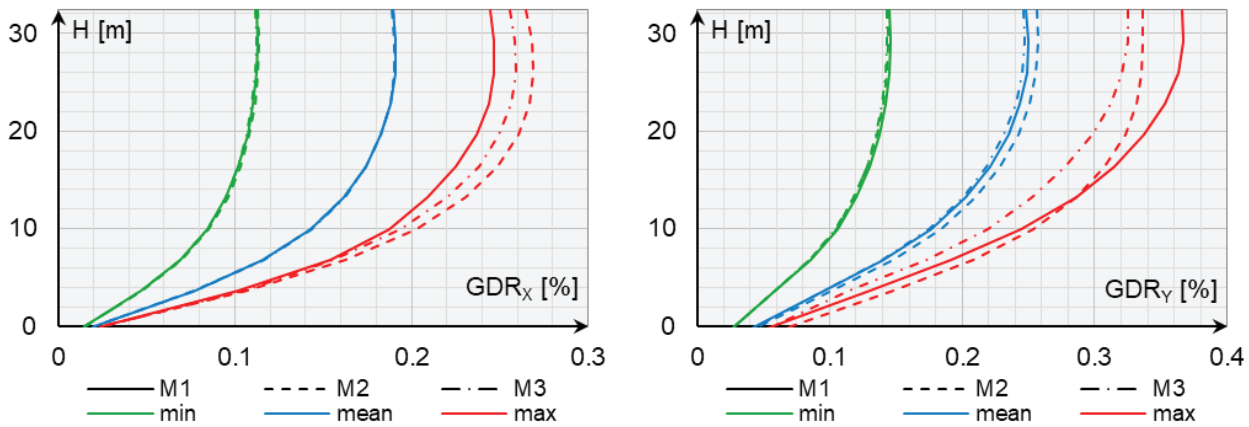

Figure 16. NDA GDR in X (left) and Y direction (right) using TH scaled data

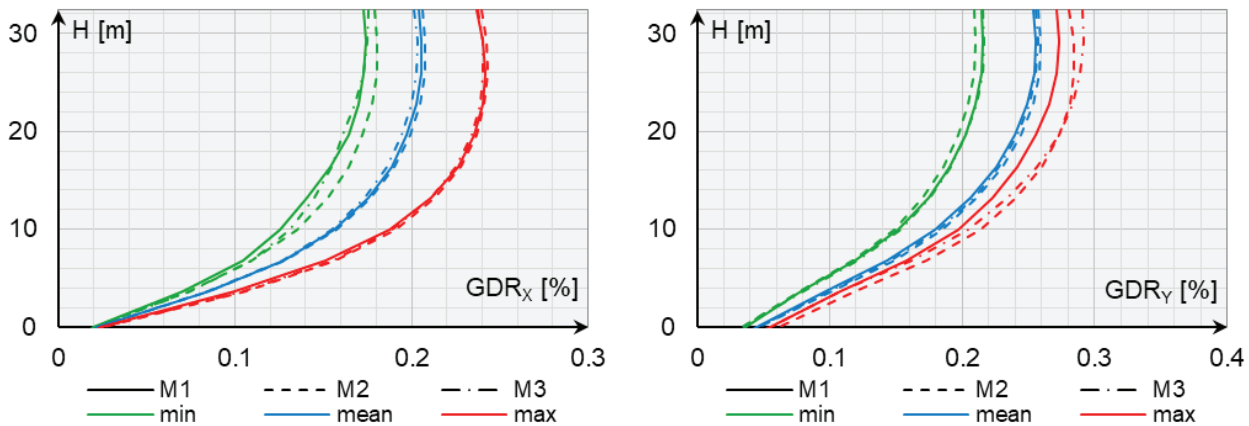

Figure 17. NDA GDR in X (left) and Y direction (right) using TH matched data

Table 6. NDA Scaled TH GDR values and their percentual difference compared to M1

GDR [%]	X dir.			Y dir.		
	min	Mean	Max	min	mean	max
M1	0.113	0.191	0.247	0.146	0.250	0.367
M2	0.114 (0.74%)	0.191 (-0.22%)	0.269 (9.04%)	0.144 (-1.23%)	0.257 (3.10%)	0.336 (-8.30%)
M3	0.112 (-0.66%)	0.191 (-0.11%)	0.259 (4.87%)	0.144 (-1.63%)	0.247 (-0.91%)	0.325 (-11.46%)

Table 7. NDA Matched TH GDR values and their percentual difference compared to M1

GDR [%]	X dir.			Y dir.		
	min	Mean	Max	min	mean	max
M1	0.174	0.206	0.242	0.216	0.255	0.273
M2	0.181 (3.81%)	0.208 (1.08%)	0.243 (0.69%)	0.210 (-2.56%)	0.259 (1.51%)	0.285 (4.28%)
M3	0.176 (0.86%)	0.203 (-1.23%)	0.241 (-0.44%)	0.217 (0.31%)	0.257 (0.68%)	0.291 (6.66%)

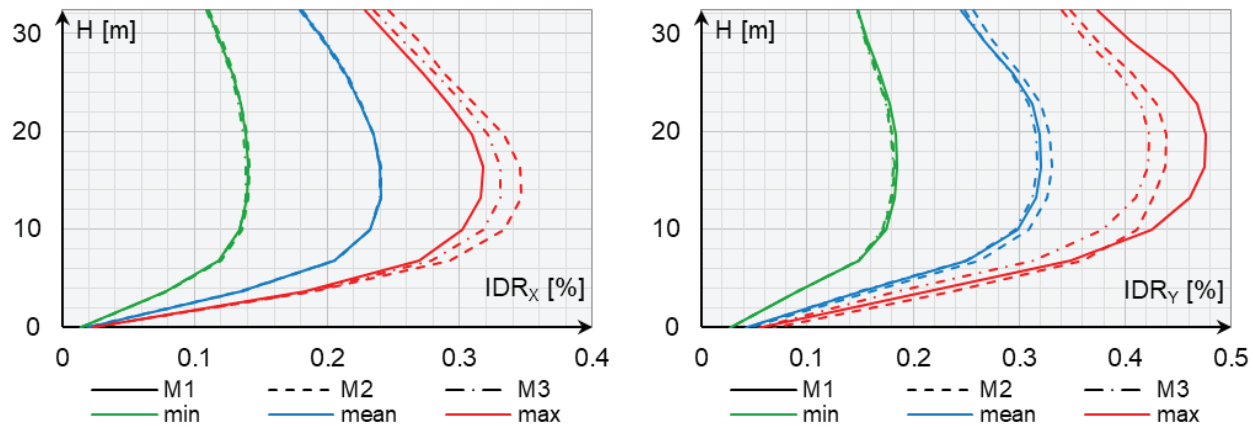

Figure 18. NDA IDR in X (left) and Y direction (right) using TH scaled data

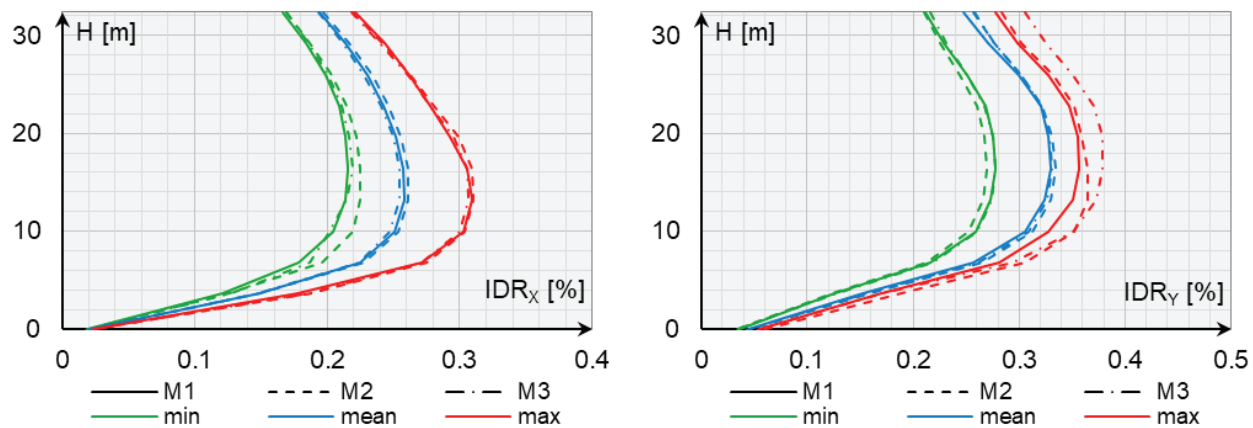

Figure 19. NDA IDR in X (left) and Y direction (right) using TH matched data

Table 8. NDA Scaled TH IDR values and their percentual difference compared to M1

GDR [%]	X dir.			Y dir.		
	min	Mean	Max	min	mean	max
M1	0.140	0.241	0.317	0.185	0.321	0.476
M2	0.141 (0.64%)	0.241 (-0.02%)	0.346 (9.05%)	0.182 (-1.46%)	0.331 (3.05%)	0.439 (-7.82%)
M3	0.139 (-0.93%)	0.240 (-0.43%)	0.331 (4.25%)	0.181 (-2.00%)	0.318 (-1.04%)	0.422 (-11.24%)

Contrary to NSA, NDA GDR percentage differences are not negligible, and their highest values amount $GDR_{X,max}^{M2} = 9.04\%$ and $GDR_{Y,max}^{M3} = -11.46\%$ for the scaled and $GDR_{X,min}^{M2} = 3.81\%$ and $GDR_{Y,max}^{M3} = 6.66\%$ for the matched TH data.

NDA GDR percentage differences and their highest values amount $IDR_{X,max}^{M2} = 9.05\%$ and $IDR_{Y,max}^{M3} = -11.24\%$ for the scaled and

Table 9. NDA Matched TH IDR values and their percentual difference compared to M1

GDR [%]	X dir.			Y dir.		
	min	Mean	Max	min	mean	max
M1	0.216	0.258	0.310	0.277	0.330	0.357
M2	0.225 (4.27%)	0.261 (1.11%)	0.310 (0.26%)	0.269 (-2.88%)	0.334 (1.36%)	0.365 (-2.27%)
M3	0.219 (1.67%)	0.254 (-1.60%)	0.306 (-1.07%)	0.277 (-0.11%)	0.331 (0.40%)	0.379 (6.20%)

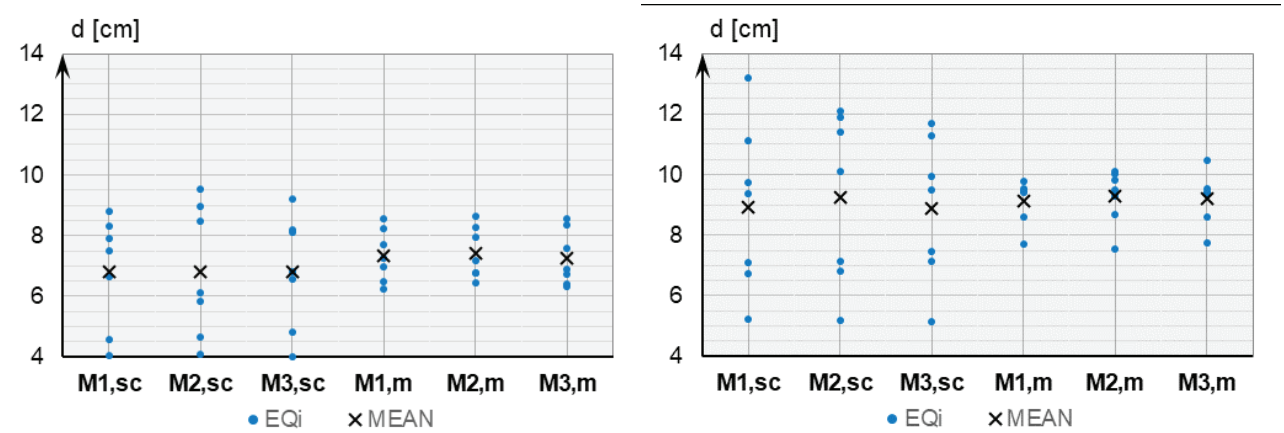

Figure 20. NDA roof displacement values in X (left) and Y direction (right) using TH scaled and matched data

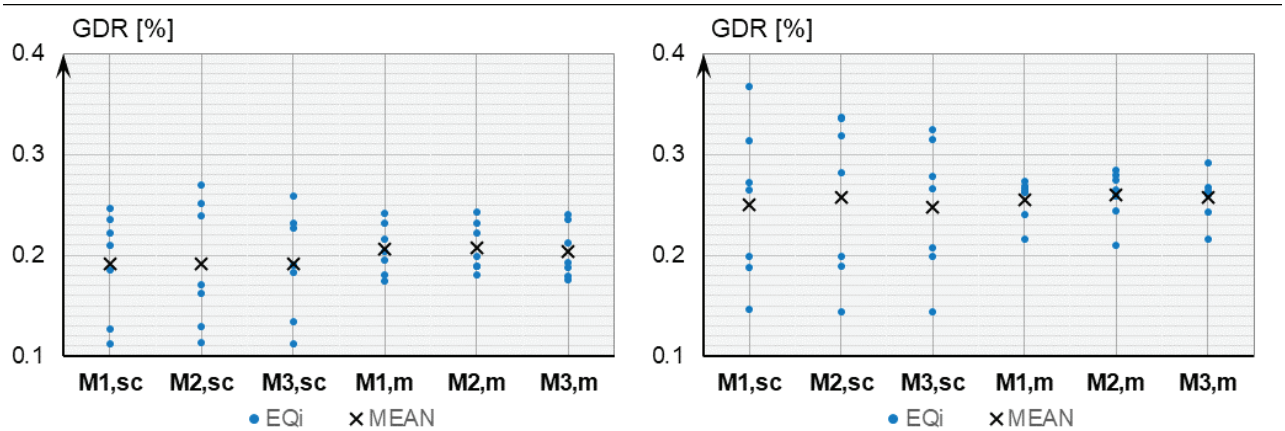

Figure 21. NDA GDR values in X (left) and Y direction (right) using TH scaled and matched data

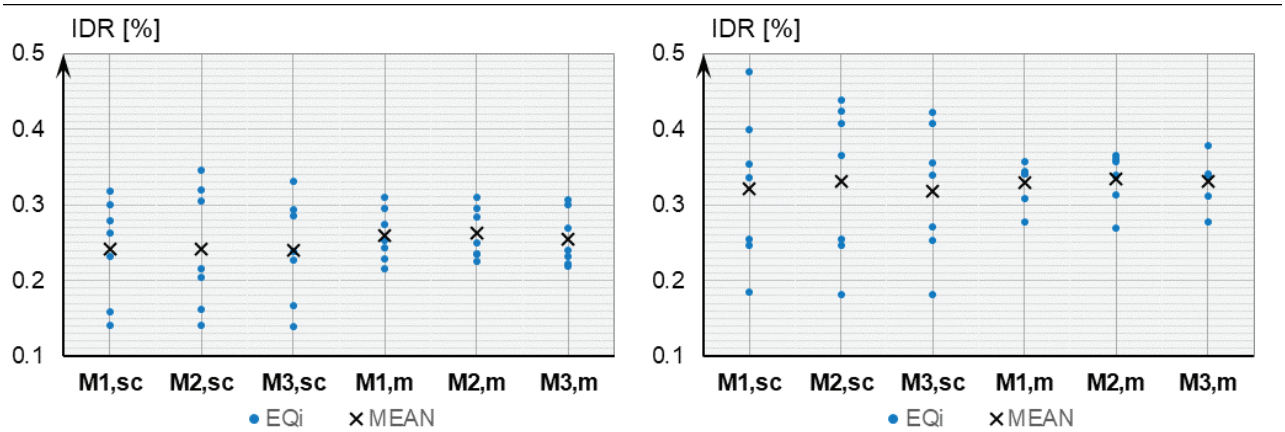

Figure 22. NDA IDR values in X (left) and Y direction (right) using TH scaled and matched data

$IDR^{M2}_{X,min} = 4.27\%$ and $IDR^{M3}_{Y,max} = 6.20\%$ for the matched TH data.

Conditions for limitation of the relative story drift (EN1998-1) are met in all three cases, i.e.:

– for buildings having non-structural elements of brittle materials attached to the structure, where: $IDR_{max} \leq \alpha/\nu = 0.005/0.5 = 1.0\%$ (Figures 18 and 19),

– for buildings having ductile non-structural elements, where: $IDR_{max} \leq \alpha/\nu = 0.0075/0.5 = 1.5\%$ (Figures 18 and 19),

– for buildings having non-structural elements fixed in a way so as not to interfere with structural deformations, or without non-structural elements, where: $IDR_{max} \leq \alpha/\nu = 0.010/0.5 = 2.0\%$ (Figures 18 and 19).

Maximum values of the roof displacements, GDR and IDR for two NDA methods in both directions for the $PGA = 0.2g$ value are calculated. The results show the wider range of the results using scaled TH data, then in case of matched TH data. In addition, the mean values are slightly higher in the second case, when the matched TH data was used. Percentage differences between M1 and models M2 and M3 are already shown in the Tables 6-9. Percentage differences between matched and scaled TH data mean values, used in two NDA cases, vary from 6.49% to 9.13% for displacements in *X* and from 0.57% to 3.82% for displacements in *Y* direction. GDR values vary from 6.45% to 7.71% in *X* and from 0.72% to 3.93% in *Y* direction. IDR values vary from 6.19% to 8.31% in *X* and from 1.00% to 4.12% in *Y* direction. The variations are a bit smaller for the values obtained for the *Y* direction.

3.2.3. Cyclic test load NDA

To analyse the differences in the behaviour of the structures in the post-elastic zone more thoroughly, the cyclic test load pattern, method B according to (ASTM E2126). However, instead of the displacement value at the ordinate and in input data, the acceleration value in *g* units was used (Figure 23).

The results of the analysis are displayed in the Figures 24-26 and compared to the already obtained pushover curves for PROP load distribution case. The results of the NDA cyclic analysis match the results of the pushover analysis with very small differences. However, beyond the displayed values, there was no convergence in the solution, so the higher values were unable to obtain.

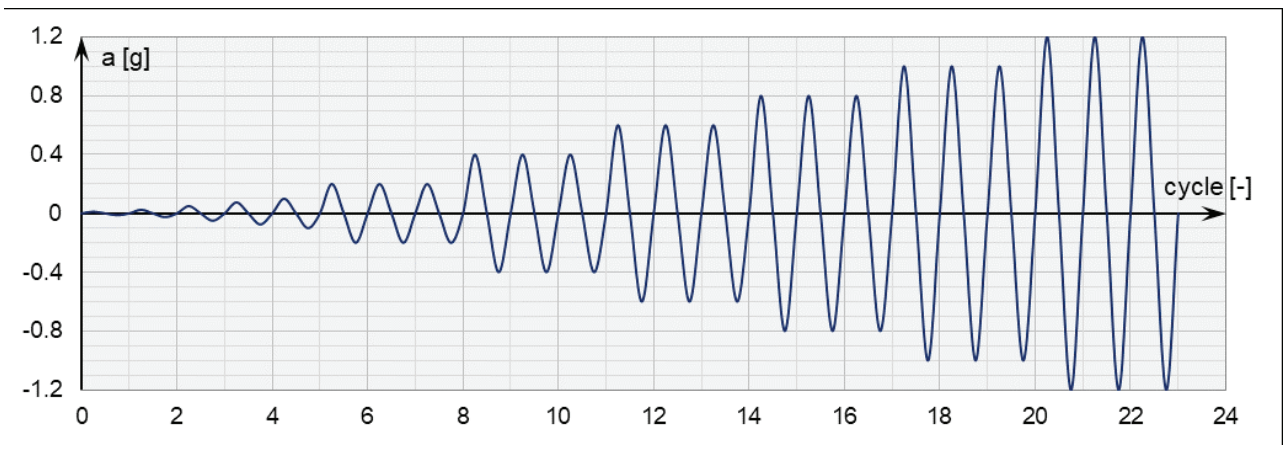

Figure 23. NDA cyclic test load pattern

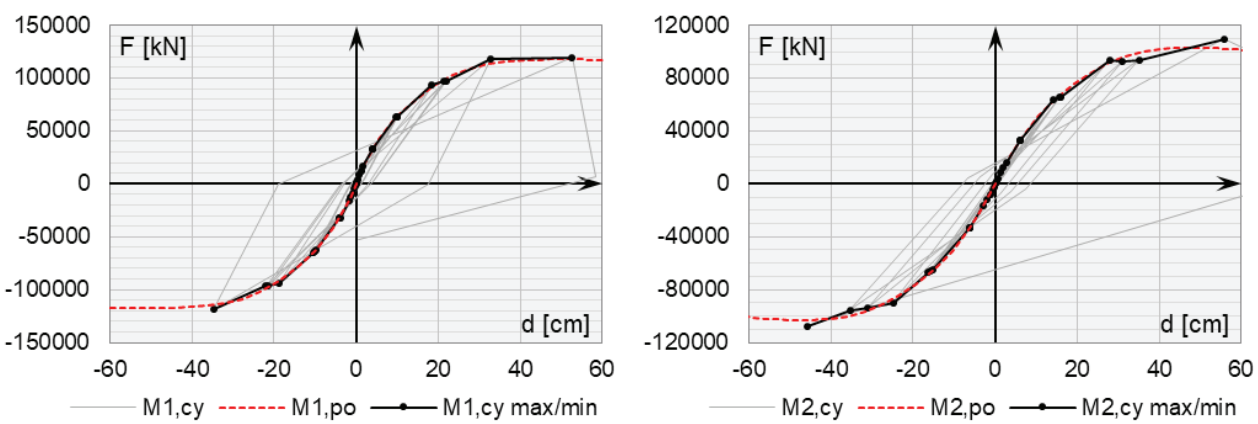

Figure 24. NDA cyclic test structural response for M1, compared to NSA pushover analysis in X (left) and Y direction (right)

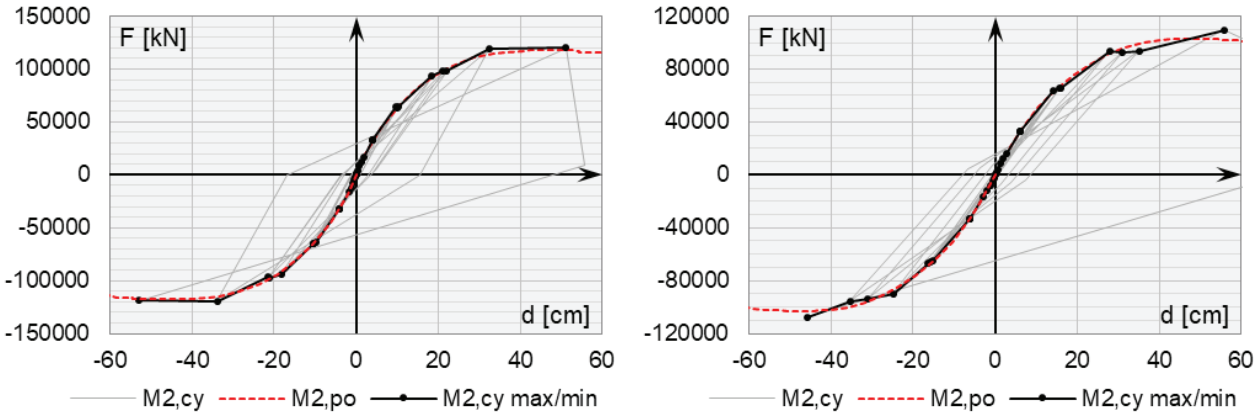

Figure 25. NDA cyclic test structural response for M1, compared to NSA pushover analysis in X (left) and Y direction (right)

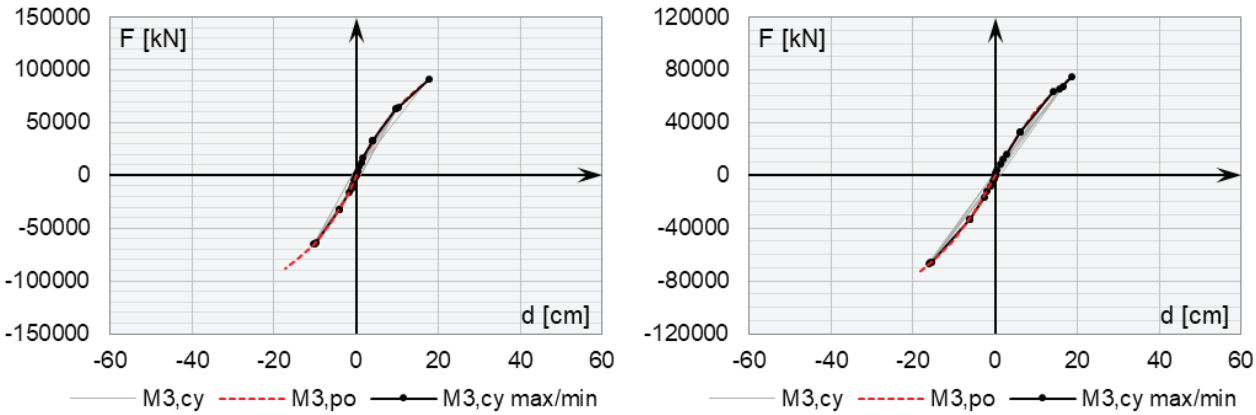

Figure 26. NDA cyclic test structural response for M1, compared to NSA pushover analysis in X (left) and Y direction (right)

3.2.3. Reinforcement amount comparison

Another parameter that is used to compare the difference between the methods of RC walls rebar detailing is the vertical flexural rebar, horizontal confining rebar and the total of the two groups. Horizontal shear rebar quantity was excluded from the comparison analysis, because it is the same in all three models. The values of M2 and M3 are compared to M1 and shown in the Table 10.

Table 10. NDA Matched TH IDR values and their percentual difference compared to M1

Model	M1	M2	M3
Vertical rebar difference [%]	/	+28.7	+28.7
Confining rebar difference [%]	/	+299.0	/
Total rebar difference [%]	/	+111.8	-27.3

Although it is already shown (through pushover, TH earthquake and cyclic load analysis) that M1 and M2 have the same structural response, the amount of rebar in RC walls in the two models is much different. Longitudinal (vertical) bars have almost 30% higher volume in M2 and M3, than in M1. In addition, since the walls in M2 are confined along its full length, the amount of confining rebar is much higher than in M1, for almost 300%. M3 lacks the confining reinforcement in RC walls, so the difference is incomparable. When summed, the difference between the total amounts is around +110% for M2 and -27.3% for M3.

4. FINAL REMARKS AND CONCLUSIONS

This paper analyses the impact of different quantity and arrangement of rebar in RC walls, which does not correspond with a typical form of RC walls with peripheral elements. (EN1998-1), (EN1992-1). Three models are considered, whereby M1 corresponds with case when seismic RC walls are designed in accordance with (EN1998-1), (EN1992-1) and it represents the reference model for a comparative analysis. Characteristics of RC walls in M2 and M3 are described in detail in the paper. Using the comparative analysis, the differences described by numerical values in the text, tables and figures from the aspect of displacements, GDR and IDR of the structural system exposed to the action of a seismic actions and cyclic load test are established. The analysis of the obtained results leads to the following conclusions:

– Using a certain quantity of rebar with atypical arrangement in RC walls in relation to (EN1998-1), (EN1992-1), the results are achieved, which can to a certain extent deviate from the results obtained by the analysis of the reference model M1.

– The M2 with the higher quantity of rebar in comparison to M1 (fully confined and evenly distributed along the wall length), will have almost the same structural response as M1. The roof displacement values, *GDR* and *IDR*, and its percentage differences compared to M1 values for the designed *PGA* and for cyclic test are very small, i.e. negligible. The only big difference is in the fact that, to achieve this kind of response, RC walls in M2 will have much higher amount of vertical and confining rebar and the total of the two.

– The M3 with the same quantity of rebar as M2 (non-confined and evenly distributed along the wall length), will have almost the same structural response as M1 for the design *PGA*. The roof displacement values, *GDR* and *IDR*, and its percentage differences compared to M1 values for the designed *PGA* are very small, i.e. negligible. However, the big difference between M3 and M1 and M3 and M2 as well, occurs in the plastic zone, after the target displacement is reached. It is established through pushover analysis and cyclic load test. The structure will lose its bearing capacity much earlier, than in other two models, with a lot less ductile response, which is which is by no means a good property. This type of response is the consequence of non-confined RC walls with much lower concrete stress limit than in confined parts of M1 and M2 RC walls that provide the ductility of the element and the structure as whole unit. As in M2, M3 walls will have much higher amount of vertical rebar, but none of the confining rebar, which will lead to the smaller total amount of the 2 types of reinforcement in RC walls in M3, compared to M1 and M2.

By analysing the results obtained from M2 and M3, it can be concluded that with the choice to use a different approach of rebar detailing in the RC walls (evenly distributed, confined and unconfined rebar), the similar response of M1 will be achieved in many of the analysed parameters (displacements, GDR and IDR for the design PGA). The differences will occur in the higher plastic zone, as it is already shown trough the results of nonlinear static pushover analysis and cyclic test load analysis. M2 will keep its properties to be the same as M1, except in the near end of its capacity, where there will be a small stiffness drop, compared to the M1. This can be seen in the results of the NSA. On the other hand, M3 will have the same response as M1 and M2, but it will reach its ultimate capacity point much earlier, because of the lack of ductile properties of its RC walls. If the relation of the results in M2 and M3 to M1 is compared, one may notice that satisfactory results with small deviations are achieved for M2, but that the structural system in M1 has a better response. (Čokić M. et al., 2021)

Based on the results of the conducted analysis, it can be concluded that the existing approach according to (EN1998-1), (EN1992-1) and the approach applied in M2 will provide the similar results in terms of the seismic structural response for adopted *PGA* and higher load intensities, but with much higher rebar quantity in M2 and economical expenses than in M1. The approach according to (EN1998-1), (EN1992-1) is strongly **recommended** in RC wall design. Providing the confined boundary elements in critical zone of the RC walls, in wall-equivalent dual structural system building, contributes to a better behaviour of the entire structural system and its seismic response.

It is established that the percentage deviations of the results in M2 and M3 are unimportant in relation to M1, but are not negligible, either. The values in M3 indicate that this approach provides the least favourable results, so irrespective of its cost-reducing potential, it **should not** be employed.

The aspect of economy is better in the case of M3, because the quantity of rebar in the walls lower, but the behaviour of the structural system in M3 is not as good as in M1, and not safe at all, so it is obvious that it **should not** be employed and it is better to use the M1 approach for walls reinforcement.

As it was mentioned, based on the analysis of considered cases, it can be assumed that with the additional increase of the quantity of rebar in M2 the same structural system response as in M1 may be achieved, but such a solution would not be economical. The approach of reinforcing of seismic RC walls used in M1 is the best approach.

Acknowledgment

The research described in this paper was financially supported by the Ministry of Education, Sciences and Development of Republic of Serbia within the Project: "A comprehensive approach to improvement of interdisciplinary researches in construction education and science" (University of Novi Sad, Faculty of Technical Sciences, Department of Civil Engineering and Geodesy) R. Folić, Z. Brujić, M. Čokić and Contract No. 451-03-9/2021-14/ 20021 (B. Folić).

REFERENCES

[1] ACI 318-11, Building Code Requirements for Structural Concrete, An ACI Standard and Commentary, Reported by ACI Committee 318, First Printing, August 2011

[2] Ajmal, M. Rahman M. K., Baluch M. H., Nonlinear Static Pushover Analysis of a Shear wall Building in Madinah, Seismic Engineering Research Infrastructures for European Synergies, 8-9 Feb. 2012, Istanbul

[3] Ajmal, M., Rahman M. K., Baluch M. H., Seismic Vulnerability of RC Shear wall Building With a Dome Roof in Moderate Seismic Region of Saudi Arabia, Arabian Journal for Science and Engineering, October 2015

[4] Ambraseys, N., Smit, P., Sigbjornsson, R., Suhadolc, P. Margaris, B., Internet-Site for European Strong-Motion Data, European Commission, Research-Directorate General, Environment and Climate Programme, 2002

[5] ASTM E2126 – 11, Standard Test Methods for Cyclic (Reversed) Load Test for Shear Resistance of Vertical Elements of the Lateral Force Resisting Systems for Buildings

[6] Avramidis, I., Athanatopoulou, A., Morfidis, K., Sextos, A., Giaralis, A., Eurocode-Compliant Seismic Analysis and Design of R/C Buildings, Concepts, Commentary and Worked Examples with Flowcharts, Springer, 2016
[7] Birely, A. et al., Investigation of the seismic behaviour and analysis of reinforced concrete structural walls, The 14th WCEE, October 12-17, 2008, Beijing, China
[8] Bisch, P., Carvalho, E., Degee, H., Fajfar, P. Fardis, M., Franchin, P., Kreslin, M., Pecker, A., Pinto, P., Plumier, A., Somja, H., Tsionis, G., Eurocode 8: Seismic Design of Buildings – Worked Examples,"EC 8: Seismic Design of Buildings" Workshop, Lisbon, 10-11 Feb. 2011
[9] Booth, E., Earthquake Design Practice for Buildings, Third edition, ICE Publishing, Thomas Telford Limited, 2014, p. 347
[10] Čokić, M. Folić, R., Seismic response of RC buildings with differently reinforced shear walls, International Scientific Conference: Earthquake Engineering and Geotechnical Aspects of Civil Engineering, 3 – 5 November 2021, Vrnjačka Banja, Serbia
[11] Ćosić, M., Brčić, S., Ground motion processing methodology for linear and nonlinear seismic analysis of structures (in Serbian), Izgradnja 66, 11–12, pp. 511–526, 2012
[12] Ćosić, M., Folić, R., Brčić, S., An Overview of Modern Seismic Analyses with Different Ways of Damping Introduction, Building Materials and Structures (60), Belgrade, Nr. 1, 2017, pp. 3-30
[13] Darani, F. M., Moghadam, A. S., Analytical Study on the Effect of Boundary Element Characteristics on the Behaviour of Low-Rise Concrete Shear Walls, 15th World Conference on Earthquake Engineering, 24-28 September 2012, Lisbon, Portugal
[14] EN1990 – Basis of structural design, CEN, 2005
[15] EN1991: Eurocode 1: Actions on structures – Part 1-1: General actions – Densities, self-weight, imposed loads for buildings, CEN, 2002
[16] EN1992 – Part 1: Eurocode 2: Design of concrete structures – Part 1-1 : General rules and rules for buildings, CEN, 2004/2005
[17] EN1998 – Part 1, Eurocode 8: Design of structures for earthquake resistance – Part 1: General rules, seismic actions and rules for buildings, CEN, 2004/2005
[18] ETABS, Computers and Structures, Inc., 2016
[19] Eurocode Standards, https://www.eurocode.us/seismic-design-eurocode-8/a-cpm.html, accessed: November 2020
[20] Fahjan, Y. M., Kubin, J., Tan, M. T., Nonlinear Analysis Methods for Reinforced Concrete Buildings With Shear Walls, 14th European Conference on Earthquake Engineering, 30 Aug. – 3 Sept. 2010, Ohrid
[21] Fahjan, Y.M., Doran, B., Akbas, B., Kubin, J., Pushover Analysis for Performance Based-Seismic Design of RC Frames With Shear Walls, 15th World Conference on Earthquake Engineering, September 24 – 28, 2012, Lisbon
[22] Fardis, M. N., Seismic Design, Assessment and Retrofitting of Concrete Buildings, based on EN-Eurocode 8, Springer, 2009, p. 743
[23] Fardis, M. N., Tsionis, G., Specific Rules for Design and Detailing of Concrete Buildings Design for DCM And DCH – Illustration Of Elements Design, Dissemination of information for training – Lisbon 10-11 February 2011
[24] Gallardo, J. A., et al. Damage and sensitivity analysis of a reinforced concrete wall building during the 2010, Chlie earthquake, Engineering Structures, 240, 2021, 112093, p. 19.
[25] Gerin, M., Adebar, P., Accounting for Shear in Seismic Analysis of Concrete Structures, 13th World Conference on Earthquake Engineering, Vancouver, B.C., Canada, August 1-6, 2004, Paper No. 1747
[26] Hagen, G. R., Performance-Based Analysis of a Reinforced Concrete Shear Wall Building, A Thesis presented to the Faculty of California Polytechnic State University for the Degree Master of Science in Architecture with a Specialization in Architectural Engineering, San Luis Obispo, June 2012
[27] Hoult, R.D., Minimum Longitudinal Reinforcement Requirements for Boundary Elements of Limited Ductile Walls for AS 3600, Electronic Journal of Structural Engineering (17), 2017
[28] Kubin, J., Fahjan Y. M., Tan, M. T., Comparison of Practical Approaches for Modelling Shearwalls in Structural Analyses of Buildings, The 14th World Conference on Earthquake Engineering, October 12-17, 2008, Beijing, China
[29] Lu, Y., Henry, R. S., Evaluation of Minimum Vertical Reinforcement Limits for Reinforced Concrete Walls, The New Zealand Concrete Industry Conference, Rotorua Convention Centre, Rotorua, New Zealand, 8-10 October 2015
[30] Mander, J., Priestley, M., Park, R.: Theoretical Stress-Strain Model for Confined Concrete, Journal of Structural Engineering, Vol. 114, iss. 8, 1988, pp. 1804-1825
[31] Menegon, S.J. et al., RC walls in Australia: seismic design and detailing to AS 1170.4 and AS 3600, Australian J. of structural Eng. 2018, Vol. 19. No. 1, 67-84
[32] Milev, J., Kardzhiev, V, Eurocodes – Guidelines for design of reinforced concrete structures – Part one: Multi-storey office building, Chamber of Engineers in Investment Design, KIIP, Regional meeting, Sofia – city, Sofia, 2012
[33] Milev, J., Problems and Their Solutions in Practical Application of Eurocodes in Seismic Design of RC Structures, Building Materials and Structures (59), Belgrade, Nr. 3, 2016, pp. 3-25
[34] NIST GCR 11-917-15, Selecting and Scaling Earthquake Ground Motions for Performing Response-History Analyses, NEHRP Consultants Joint Venture for U.S. Department of Commerce National Institute of Standards and Technology Engineering Laboratory Gaithersburg, Maryland, November 2011
[35] Oh, Y-H., Han, S. W., Lee, L-H, Effect of boundary element details on the seismic deformation capacity of structural walls, Earthquake Engineering and Structural Dynamics, 2002; 31:1583–1602 (DOI: 10.1002/eqe.177)
[36] ORFEUS, Engineering Strong Motion Database, https://esm-db.eu/, accessed: November 2020
[37] Paulay, T., Priestley, M.J.N., Seismic Design of Reinforced Concrete and Masonry Buildings, John Wiley and Sons, New York, U.S.A., 1992, pp. 767
[38] Rana, R., Jin, L., Zekioglu, A., Pushover Analysis of a 19 Story Concrete Shear Wall Building, 13th World Conference on Earthquake Engineering, Vancouver, B.C., Canada, August 1-6, 2004, Paper No. 133
[39] SeismoMatch, Seismosoft, 2018
[40] Sukumar, B., Hemamathi, A., Kokila, S., Hanish, C., A Comparative Study on Nonlinear Analysis of Frame With and Without Structural Wall System, SSRG International Journal of Civil Engineering, Volume 3, Issue 3, March 2016
[41] Zhao, X., Wu, Y.-F., Leung, A.Y., Lam H. F., Plastic Hinge Length in Reinforced Concrete Flexural Members, Available online at www.sciencedirect.com The Twelfth East Asia-Pacific Conference on Structural Engineering and Construction, Procedia Engineering 14 (2011) 1266–1274